Multiple band structures in ^{169,170}Re: Search for the wobbling mode in ^{169}Re, and residual-interaction analysis of structures in ^{170}Re

D. J. Hartley,[1] R. V. F. Janssens,[2] L. L. Riedinger,[3] M. A. Riley,[4] X. Wang,[4] S. Miller,[4] A. D. Ayangeakaa,[5] P. F. Bertone,[2] M. P. Carpenter,[2] C. J. Chiara,[2,6,7] P. Chowdhury,[8] U. Garg,[5] G. Gürdal,[7] S. S. Hota,[8] F. G. Kondev,[7] T. Lauritsen,[2] W. C. Ma,[9] J. Matta,[5] E. A. McCutchan,[2,*] S. Mukhopadhyay,[5,†] E. E. Pedicini,[1,‡] J. R. Vanhoy,[1] and S. Zhu[2]

[1]*Department of Physics, US Naval Academy, Annapolis, Maryland 21402, USA*
[2]*Physics Division, Argonne National Laboratory, Argonne, Illinois 60439, USA*
[3]*Department of Physics and Astronomy, University of Tennessee, Knoxville, Tennessee 37996, USA*
[4]*Department of Physics, Florida State University, Tallahassee, Florida 32306, USA*
[5]*Department of Physics, University of Notre Dame, Notre Dame, Indiana 46556, USA*
[6]*Department of Chemistry and Biochemistry, University of Maryland, College Park, Maryland 20742, USA*
[7]*Nuclear Engineering Division, Argonne National Laboratory, Argonne, Illinois 60439, USA*
[8]*Department of Physics, University of Massachusetts Lowell, Lowell, Massachusetts 01854, USA*
[9]*Department of Physics, Mississippi State University, Mississippi State, Mississippi 39762, USA*

(Received 29 November 2012; published 20 February 2013)

Although the observation of wobbling was once thought to be possibly confined to lutetium isotopes in $N \approx 94$ nuclei, the identification of this exotic collective mode in ^{167}Ta has raised the question of the role of the proton Fermi surface with regard to this phenomenon. To investigate this issue, an experiment was performed to populate high-spin states in the $N = 94$ nucleus ^{169}Re. The heavy-ion reaction ^{55}Mn + ^{118}Sn was used in conjunction with Gammasphere to detect the emitted γ rays. More than 130 new transitions were added to the ^{169}Re level scheme, including the first identification of the $\pi i_{13/2}$ rotational sequence in this nucleus. This configuration is the structure on which all known wobbling sequences are based, but no wobbling band was observed, likely owing to the fact that the $\pi i_{13/2}$ sequence is located at a relatively high energy in comparison with the other structures found in ^{169}Re. Nine decay sequences are now established in this nucleus and are described within the context of the cranked shell model. In addition, significant extension of the level scheme of the odd-odd ^{170}Re nucleus was possible and a discussion of the residual interactions for the $\pi h_{9/2}\nu i_{13/2}$ and $\pi i_{13/2}\nu i_{13/2}$ configurations in this region is given as well.

DOI: 10.1103/PhysRevC.87.024315 PACS number(s): 21.10.Re, 23.20.Lv, 27.70.+q

I. INTRODUCTION

The identification of the wobbling mode is perhaps the best experimental signature for the existence of stable triaxial deformation. This is attributable to the fact that such a sequence can only occur for rotating asymmetric nuclear shapes. First found in ^{163}Lu [1], wobbling bands were observed soon after in ^{165,167}Lu [2,3] and, possibly, ^{161}Lu [4]. Despite numerous searches in neighboring nuclei, no other examples could be found for many years, leading to the suggestion that lutetium may be the only species to exhibit this exotic phenomenon in the $Z \approx 72$, $N \approx 94$ region [5]. However, the recent identification of a candidate wobbling sequence in the $N = 94$ nucleus ^{167}Ta [6,7] indicates that the region for observing this collective mode extends beyond lutetium. It also aids in the confirmation of the $N = 94$ triaxial strongly deformed shell gap predicted in Ref. [8]. Therefore, the role of the proton Fermi surface, with regards to wobbling, should be explored. With this motivation, an experiment on the $N = 94$ nucleus ^{169}Re was conducted to search for the wobbling mode.

All wobbling structures in this region are based on the $\pi i_{13/2}$ band. This configuration was not observed in an earlier high-spin study of ^{169}Re [9], but was identified in the present work, together with eight other bands. Unfortunately, a wobbling band was not observed and a discussion of its absence is presented. The level scheme for ^{169}Re was greatly extended and configuration assignments are proposed for the observed bands through the analysis of alignments, band crossings, and $B(M1)/B(E2)$ ratios. In addition, a new band could be associated with the odd-odd nucleus ^{170}Re [10] and the previously known sequence was extended to higher spins. A systematic investigation into the residual interactions of the $\pi h_{9/2}\nu i_{13/2}$ and the $\pi i_{13/2}\nu i_{13/2}$ configurations was also performed.

II. EXPERIMENTAL DETAILS

The reaction ^{55}Mn + ^{118}Sn was selected to populate excited states of ^{169}Re and ^{170}Re with the $4n$ and $3n$ fusion-evaporation channels, respectively. The ATLAS facility at Argonne National Laboratory provided the 260-MeV ^{55}Mn beam with a current of $\sim$2 pnA throughout the experiment. Two stacked ^{118}Sn targets, each with 0.6 mg/cm^2 thickness, were bombarded by this beam for a period of approximately 6 days. Emitted γ rays were detected with the Gammasphere spectrometer [11] consisting of 101 Compton-suppressed Ge detectors. A total of 2.3×10^9 fourfold or greater coincidence events were recorded and sorted into a Blue database [12].

*Present address: National Nuclear Data Center, Brookhaven National Laboratory, Upton, New York 11973-5000.
†Present address: Nuclear Physics Division, Bhabha Atomic Research Center, Mumbai 400085, India.
‡Present address: Department of Nuclear Engineering, Texas A & M University, College Station, Texas 77843.

Radware [13] coincidence cubes and hypercubes were built and an angular-correlation analysis was performed with this database. The latter was performed in the following manner. A coincidence of two known quadrupole γ rays in an event was required, and the other coincident transitions within the same event were sorted into 16 separate spectra (corresponding to each of the 16 available rings of detectors). Background subtraction was performed with the method described by K. Starosta *et al.* [14]. Spectra from the five rings nearest 90° ($\theta = 79°, 81°, 90°, 99°$, and 101°) were summed together, and the intensities of resultant peaks, $W(\theta_{90°})$, were determined. Similarly, the intensities of the same peaks at backward angles, $W(\theta_b)$, were obtained with rings located at $\theta = 122°$, 130°, 143°, 148°, and 163°. A ratio of the intensities, $R_{\rm ang} = W(\theta_b)/W(\theta_{90°})$, was calculated and normalized such that known pure dipole and quadrupole transitions had values of 0.6 and 1.0, respectively. Information on the observed states and γ rays have been tabulated in Table I.

III. LEVEL SCHEME: ^{169}Re

Two decay studies [15,16] of ^{169}Re were published in 1992 and reported two states that β^+ decay in addition to weak α branches. An evaluation of the ^{169}Re data [17] suggested that the $I^\pi = (9/2^-)$ ($t_{1/2} = 8.1$ s) level is the ground state, while systematics suggest that the $(5/2^+,3/2^+)$ ($t_{1/2} = 15.1$ s) state is an isomer. Recently, Zhou *et al.* [9] presented three rotational bands in ^{169}Re. Connections between two of the bands were observed, leaving the third with an unknown relative energy. States as high as spin $I = 45/2$ were populated in this study.

In the present work, an extensive level scheme was constructed as displayed in Fig. 1. Nine structures are now observed, where the highest spin state is 77/2. All of these sequences are connected such that the relative excitation energies are known. The lowest observed state has been associated with a spin/parity of $9/2^-$, consistent with the evaluated assignment for the ground state [17]. In all, five additional rotational sequences and more than 130 new transitions have been added to the ^{169}Re level scheme.

A. Band 1

Band 1 in Fig. 1 was previously observed in Ref. [9] up to a spin of 45/2 and was suggested to be based on the ground state. In the present data, the bandhead state was indeed found to be the lowest observed level, such that it likely corresponds to the proposed $(9/2^-)$ ground state suggested in Refs. [9,17]. This sequence was extended to 63/2 as evidenced by the spectrum of Fig. 2(a) that was produced by a sum of many triple gates in the hypercube. At lower spins, band 1 is the yrast sequence, as can be ascertained from Fig. 3, which provides the energy of the observed states minus a rigid-rotor reference. The configuration assignment for band 1 discussed in Ref. [9], as well as in Sec. V A, strongly indicates that this structure is of negative parity.

B. Band 2

A new, strongly coupled band was observed in the present data feeding into band 1 and has been labeled as band 2 in

TABLE I. γ-ray energies and intensities in ^{169}Re.

I^{π}[a]	$E_{\rm level}$ (keV)	E_γ (keV)[b]	I_γ[c]	Angular correlation ratio
		Band 1: [514]9/2 $\alpha = +1/2$		
$\frac{9}{2}^-$	0.0			
$\frac{13}{2}^-$	382.7	382.7	∼31[e]	0.76(5)
		246.3	∼131[e]	0.78(2)
$\frac{17}{2}^-$	940.0	557.3	43(4)	1.03(5)
		317.6	72(4)	0.79(5)[f]
$\frac{21}{2}^-$	1583.9	643.9	45(4)	0.81(5)
		365.4	41(3)	0.86(4)
$\frac{25}{2}^-$	2257.7	673.8	30(2)	0.89(8)
		375.4	27(2)	0.76(4)
$\frac{29}{2}^-$	2602.7	345.0	2.7(8)	
		116.0	20(1)	0.60(4)
$\frac{33}{2}^-$	2923.7	321.0	4.0(9)	
		180.2	35(2)	0.65(2)
$\frac{37}{2}^-$	3396.2	472.5	9(1)	1.00(8)
		255.2	38(2)	0.73(3)
$\frac{41}{2}^-$	4005.7	609.5	14(1)	
		319.1	25(1)	0.79(5)[f]
$\frac{45}{2}^-$	4727.1	721.4	9.2(6)	
		371.2	10(1)	0.75(6)
$\frac{49}{2}^-$	5537.5	810.4	4.1(3)	
		412.3	3.7(4)	0.87(9)
$\frac{53}{2}^-$	6413.8	876.3	2.4(3)	
		440.7	2.1(3)	
$\frac{57}{2}^-$	7312.7	898.9	1.6(2)	
		443.4	1.0(2)	
$\frac{61}{2}^-$	8185.5	872.8	0.8(1)	
		429.7	0.6(1)	
		Band 1: [514]9/2 $\alpha = -1/2$		
$\frac{11}{2}^-$	136.4	136.4	∼79[d]	0.67(3)
$\frac{15}{2}^-$	622.4	486.0	67(5)	0.86(4)
		239.8	≡100	0.81(3)
$\frac{19}{2}^-$	1218.4	596.0	74(5)	0.9(1)
		278.4	48(3)	0.74(3)
$\frac{23}{2}^-$	1882.2	663.8	59(4)	1.01(4)
		298.3	30(2)	0.70(5)
$\frac{27}{2}^-$	2486.7	604.5	46(3)	0.79(4)
		229.1	33(2)	0.67(3)
$\frac{31}{2}^-$	2743.6	140.9	27(2)	0.59(3)
$\frac{35}{2}^-$	3141.1	397.5	6.3(6)	0.9(1)[f]
		217.4	39(2)	0.66(2)
$\frac{39}{2}^-$	3686.5	545.4	10.5(6)	1.02(8)
		290.4	36(3)	0.70(3)
$\frac{43}{2}^-$	4355.9	669.4	7.9(5)	
		350.3	18(1)	0.72(5)
$\frac{47}{2}^-$	5125.1	769.2	5.4(3)	
		398.0	6.5(5)	0.9(1)[f]
$\frac{51}{2}^-$	5973.0	847.9	2.9(4)	
		435.7	2.5(4)	
$\frac{55}{2}^-$	6869.4	896.4	2.1(2)	
		455.4	1.2(1)	
$\frac{59}{2}^-$	7755.9	886.5	1.4(1)	
		443.0	0.5(1)	
$\frac{63}{2}^-$	8626.3	870.4	0.6(1)	

TABLE I. (*Continued*.)

I^{π} [a]	E_{level} (keV)	E_{γ} (keV)[b]	I_{γ} [c]	Angular correlation ratio
		Band 2: $\pi h_{11/2}AF\ \alpha = +1/2$		
$(\frac{37}{2}^+)$	3946.8	805.6	0.7(1)	
$(\frac{41}{2}^+)$	4533.2	586.4	0.7(1)	
		846.7	3.6(4)	
$(\frac{45}{2}^+)$	5079.6	546.4	0.7(1)	
		281.2	4.0(3)	
$(\frac{49}{2}^+)$	5732.3	652.7	1.3(1)	
		343.2	2.0(1)	
$(\frac{53}{2}^+)$	6516.4	784.1	1.0(1)	
		411.1	1.0(1)	
$(\frac{57}{2}^+)$	7398.2	881.8	0.5(1)	
		453.4	0.5(1)	
$(\frac{61}{2}^+)$	(8316)	(918)	<0.3	
		Band 2: $\pi h_{11/2}AF\ \alpha = -1/2$		
$(\frac{39}{2}^+)$	4297			
$(\frac{43}{2}^+)$	4798.4	501	<0.3	
		265.2	3.7(4)	
$(\frac{47}{2}^+)$	5389.0	590.6	1.1(1)	
		309.4	2.9(2)	
$(\frac{51}{2}^+)$	6105.2	716.2	1.1(1)	
		372.9	1.5(1)	
$(\frac{55}{2}^+)$	6944.9	839.7	0.8(1)	
		428.6	0.8(1)	
$(\frac{59}{2}^+)$	(7838)	(893)	<0.3	
		Band 3 $\alpha = +1/2$		
$(\frac{17}{2}^+)$	1623.4	280.5	11(1)	0.61(5)
		113.4	0.5(1)	
		191.4	6(1)	0.78(9)[f]
		404.9	12(1)	0.58(8)
		683.4	6.4(6)	0.75(6)
		1000.9	5.7(4)	0.52(5)
$(\frac{21}{2}^+)$	1991.6	368.2	3.0(4)	
		192.3	14(3)	0.78(9)[f]
		773.0	0.4(1)	
		Band 3 $\alpha = -1/2$		
$(\frac{15}{2}^+)$	1342.9	720.5	14(1)	0.76(6)
		960.2	5.5(5)	0.41(5)
$(\frac{19}{2}^+)$	1799.3	175.9	25(3)	0.65(9)[f]
		215.3	1.0(2)	
		367.5	1.6(3)	
		859.3	3.7(3)	0.74(5)
		Band 4: $\pi h_{11/2}AE\ \alpha = -1/2$		
$(\frac{23}{2}^+)$	2183.5	191.9	15(2)	0.78(9)[f]
		(61)		
		384.2	3.2(5)	
$(\frac{27}{2}^+)$	2462.1	155.6	16(1)	0.63(5)
$(\frac{31}{2}^+)$	2896.4	434.3	4.6(5)	
		238.7	21(3)	0.68(8)[f]
$(\frac{35}{2}^+)$	3464.7	568.3	8.3(8)	0.91(5)
		294.8	17(2)	0.65(4)
$(\frac{39}{2}^+)$	4106.5	641.8	7.4(6)	1.03(6)[f]
		314.4	11(1)	0.56(9)[f]
$(\frac{43}{2}^+)$	4728.2	621.7	6.0(5)	0.99(6)[f]
		294.2	8(1)	0.66(6)[f]

TABLE I. (*Continued*.)

I^{π} [a]	E_{level} (keV)	E_{γ} (keV)[b]	I_{γ} [c]	Angular correlation ratio
$(\frac{47}{2}^+)$	5298.7	570.5	5.6(5)	0.91(5)
		282.9	6.0(8)	0.61(5)
$(\frac{51}{2}^+)$	5912.1	613.4	3.2(4)	
		317.0	5.0(6)	0.56(9)[f]
$(\frac{55}{2}^+)$	6615.6	703.5	2.1(2)	
		366.6	3.9(3)	
$(\frac{59}{2}^+)$	7416.4	800.8	1.3(1)	
		417.5	1.7(1)	
$(\frac{63}{2}^+)$	8311.6	895.2	1.0(1)	
		467.9	0.6(2)	
$(\frac{67}{2}^+)$	9295.7	984.1	<0.3	
		Band 4: $\pi h_{11/2}AE\ \alpha = +1/2$		
$(\frac{21}{2}^+)$	2122.8	323.6	1.6(2)	
		690.9	2.1(3)	
$(\frac{25}{2}^+)$	2306.5	123.0	12(1)	0.61(8)
$(\frac{29}{2}^+)$	2657.7	351.2	3.6(3)	
		195.5	19(2)	0.71(5)
$(\frac{33}{2}^+)$	3169.7	512.0	4.8(4)	
		273.3	19(1)	0.67(5)
$(\frac{37}{2}^+)$	3792.2	622.5	7.9(7)	0.99(6)[f]
		327.6	13(2)	
$(\frac{41}{2}^+)$	4434.1	641.9	6.7(8)	1.03(6)[f]
		327.5	9(1)	
$(\frac{45}{2}^+)$	5015.7	581.6	5.9(8)	1.07(9)[f]
		287.5	7.1(8)	0.60(5)
$(\frac{49}{2}^+)$	5595.0	579.3	3.3(4)	1.07(9)[f]
		296.4	5.7(5)	0.66(6)[f]
$(\frac{53}{2}^+)$	6248.9	653.9	2.5(2)	
		337.0	4.5(4)	
$(\frac{57}{2}^+)$	6998.8	749.9	1.8(1)	
		383.4	2.8(2)	
$(\frac{61}{2}^+)$	7843.6	844.8	1.0(1)	
		427.3	1.3(1)	
$(\frac{65}{2}^+)$	8778.5	934.9	0.7(1)	
		467.0	0.5(2)	
		Band 5: [402]5/2 $\alpha = +1/2$		
$(\frac{5}{2}^+)$	119.0			
$(\frac{9}{2}^+)$	447.9	328.9	1.6(2)	
		176.3	9.1(9)	
$(\frac{13}{2}^+)$	898.0	450.1	5.1(5)	
		260.4	8.2(7)	
$(\frac{17}{2}^+)$	1431.9	533.9	5.4(5)	
		310.2	6.3(6)	
		Band 5: [402]5/2 $\alpha = -1/2$		
$(\frac{7}{2}^+)$	271.4	152.5	6.8(5)	
$(\frac{11}{2}^+)$	637.6	366.2	3.6(3)	
		189.9	8.5(9)	
$(\frac{15}{2}^+)$	1121.7	484.1	4.9(4)	
		223.7	8.0(6)	
		Band 6: [541]1/2 $\alpha = +1/2$		
$\frac{5}{2}^-$	536.0	320.1	∼10[e]	0.71(3)
$\frac{9}{2}^-$	633.8	97.8	3.0(4)	0.7(1)
		355.0	1.4(2)	0.6(1)
		497.4	5.9(8)	0.96(5)

TABLE I. (*Continued.*)

I^{π} [a]	E_{level} (keV)	E_{γ} (keV)[b]	I_{γ} [c]	Angular correlation ratio
		633.8	1.7(2)	
$\frac{13}{2}^-$	886.9	253.1	17(1)	0.82(2)
		886.8	1.6(2)	0.9(1)
$\frac{17}{2}^-$	1275.7	388.8	17(2)	0.89(2)
$\frac{21}{2}^-$	1764.9	489.2	15(1)	0.87(2)
$\frac{25}{2}^-$	2321.2	556.3	14(2)	0.99(5)[f]
$\frac{29}{2}^-$	2903.7	582.5	13(2)	1.10(3)
$\frac{33}{2}^-$	3458.6	554.9	13(2)	0.99(5)[f]
$\frac{37}{2}^-$	3942.8	484.2	11(1)	1.06(5)
$\frac{41}{2}^-$	4452.3	509.5	9.5(9)	1.03(3)
$\frac{45}{2}^-$	5048.8	596.5	8.6(6)	0.96(3)
$\frac{49}{2}^-$	5727.0	678.2	6.8(4)	1.02(4)
$\frac{53}{2}^-$	6466.7	739.7	5.4(4)	1.24(6)
$\frac{57}{2}^-$	7248.3	781.6	3.2(3)	1.12(7)
$\frac{61}{2}^-$	8062.3	814.0	1.9(2)	1.2(1)
$\frac{65}{2}^-$	8918.8	856.5	0.9(1)	
$\frac{69}{2}^-$	9812.8	894.0	0.4(1)	
$\frac{73}{2}^-$	10756.0	943.2	<0.3	
$\frac{77}{2}^-$	11765	1009	<0.3	
		Band 6a		
	8024.2	775.9	<0.3	
	8861.7	837.5	<0.3	
		799.3	<0.3	
	9744	880	<0.3	
		Band 7		
$\frac{37}{2}^-$	4164.5	705.9	1.0(1)	0.98(5)
$\frac{41}{2}^-$	4746.1	581.6	0.8(1)	
		803.3	0.3(1)	1.05(7)
$\frac{45}{2}^-$	5377.7	631.6	1.0(1)	
$\frac{49}{2}^-$	6061.5	683.8	0.7(1)	
$\frac{53}{2}^-$	6812.5	751.0	0.5(1)	
$\frac{57}{2}^-$	7635.4	822.9	0.3(1)	
		Band 8: [660]1/2		
$\frac{17}{2}^+$	1663.4	1041.0	3.2(4)	0.71(9)
		387.8	0.8(2)	
$\frac{21}{2}^+$	2038.3	374.9	3.3(4)	0.9(1)
$\frac{25}{2}^+$	2497.9	459.6	2.4(2)	1.0(1)
$\frac{29}{2}^+$	3025.4	527.5	1.1(1)	0.92(8)
		516.0	0.8(1)	
$\frac{33}{2}^+$	3608.1	582.7	1.7(2)	1.2(1)
$\frac{37}{2}^+$	4238.0	629.9	1.4(2)	0.9(2)[f]
$\frac{41}{2}^+$	4867.1	629.1	1.1(2)	0.9(2)[f]
$\frac{45}{2}^+$	5426.3	559.2	1.0(1)	1.1(1)
$\frac{49}{2}^+$	6056.5	630.2	0.6(1)	0.9(2)[f]
$\frac{53}{2}^+$	6743.0	686.5	0.5(1)	
$\frac{57}{2}^+$	7494.3	751.3	<0.3	
$\frac{61}{2}^+$	8298.5	804.2	<0.3	
$(\frac{65}{2}^+)$	(9138)	(839)	<0.3	

TABLE I. (*Continued.*)

I^{π} [a]	E_{level} (keV)	E_{γ} (keV)[b]	I_{γ} [c]	Angular correlation ratio
		Band 9: $\pi h_{9/2}AE$		
$\frac{27}{2}^+$	3083.7	574.4	<0.3	
		585.7	<0.3	
		597.0	<0.3	
		762.9	<0.3	
$\frac{31}{2}^+$	3344.2	260.5	1.5(2)	
		423.3	<0.3	
		440.8	0.3(1)	
$\frac{35}{2}^+$	3720.0	375.8	2.4(3)	
$\frac{39}{2}^+$	4219.7	499.7	1.9(2)	
		823.4	0.4(1)	
$\frac{43}{2}^+$	4836.8	617.1	2.4(2)	
$\frac{47}{2}^+$	5545.7	708.9	1.9(2)	
$\frac{51}{2}^+$	6315.3	769.6	1.7(2)	
$\frac{55}{2}^+$	7063.9	748.6	1.3(1)	
$\frac{59}{2}^+$	7785.3	721.4	1.0(1)	
$\frac{63}{2}^+$	8554.1	768.8	0.8(1)	
$\frac{67}{2}^+$	9395.8	841.7	0.4(1)	
$\frac{71}{2}^+$	10306.9	911.1	<0.3	
$\frac{75}{2}^+$	11286	979	<0.3	
		Other levels and γ rays		
$\frac{3}{2}$	215.9			
$\frac{7}{2}$	278.8			
	1510.0	887.6	0.3(1)	
	1510.0	1127.3	<0.3	
$(\frac{25}{2}^+)$	2509.4	471.0	1.0(2)	
	2920.9	663.3	0.3(1)	

[a]Spin and parity of the depopulated state.
[b]Uncertainties in γ-ray energy are 0.2 keV for most transitions, except for relatively weak transitions ($I_{\gamma} < 0.3$), where 0.5-keV uncertainties are appropriate.
[c]Relative intensity of the transition with respect to the intensity of the 239.8-keV transition.
[d]Estimated based on intensity balance.
[e]Estimated based on intensity balance and branching ratio.
[f]Unresolved doublet.

Fig. 1. Two linking transitions were found to feed the 35/2 and 39/2 states of band 1. The coincidence between bands 1 and 2 can be clearly seen in the example spectrum for band 2 in Fig. 2(b), where the peaks labeled with squares are transitions from band 1. Unfortunately, a reliable angular-correlation ratio could not be determined for either of the linking transitions. However, based on the intensity of the sequence (slightly less than band 1 at similar spins), the linking transitions are tentatively assigned as $\Delta I = 1$ in order for band 2 to lie slightly higher in energy than band 1 at higher spins [see Fig. 3(a)]. Positive parity is suggested for band 2 based on the configuration assignment discussed in Sec. V B. No distinct transitions could be associated with the decay out of the 39/2 state, indicating that many deexcitation paths are likely involved with intensities below the sensitivity of the present experiment.

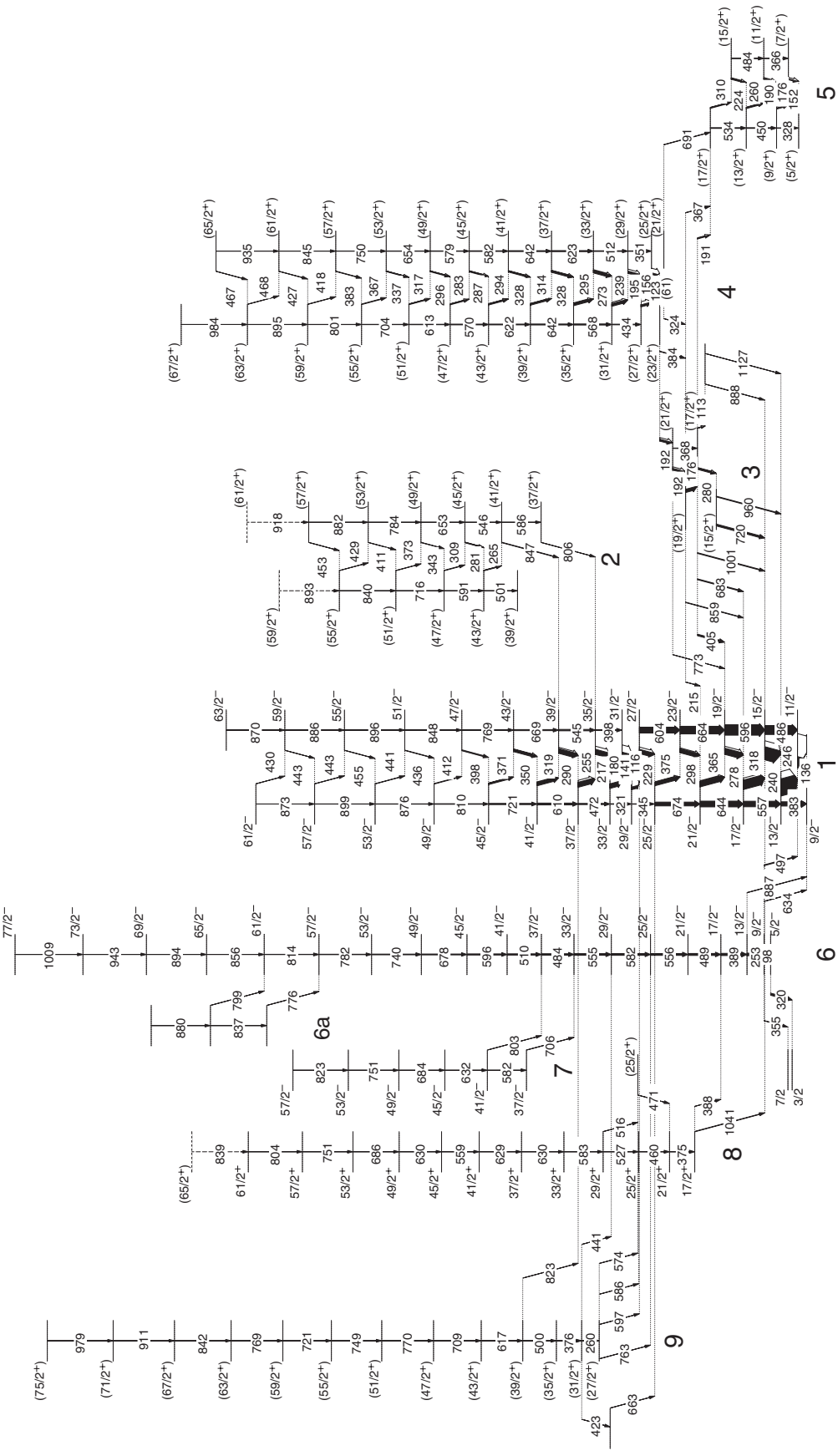

FIG. 1. Level scheme for ^{169}Re from the present analysis. The widths of the arrows are proportional to the relative intensities of the γ rays. Tentative levels and γ rays are shown as dashed lines.

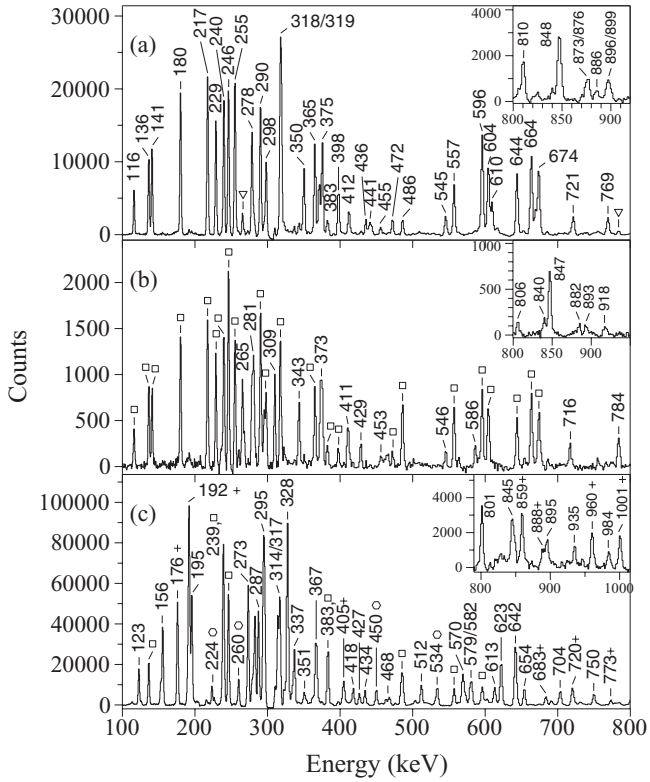

FIG. 2. (a) Spectrum for band 1 in ^{169}Re. Both the main spectrum and the inset result from a sum of all the possible triple combinations of coincidence gates in the hypercube where any of the 136-, 246-, or 240-keV transitions were in coincidence with any two dipole transitions between the 25/2 and 45/2 levels. The peaks denoted with upside-down triangles are from band 2. (b) Spectrum for band 2. All possible triple combinations of the dipole transitions between the 25/2 and 39/2 states in band 1 with any two dipole γ rays between the (41/2) and (49/2) levels in band 2 produced both the main spectrum and the high-energy inset. Peaks denoted with squares are coincident transitions from band 1. (c) Spectrum for band 4. All possible triple combinations of the dipole transitions between the 23/2 and 47/2 levels were summed to produce both spectra. Peaks denoted with a square, plus, and hexagon are transitions from bands 1, 3, and 5, respectively.

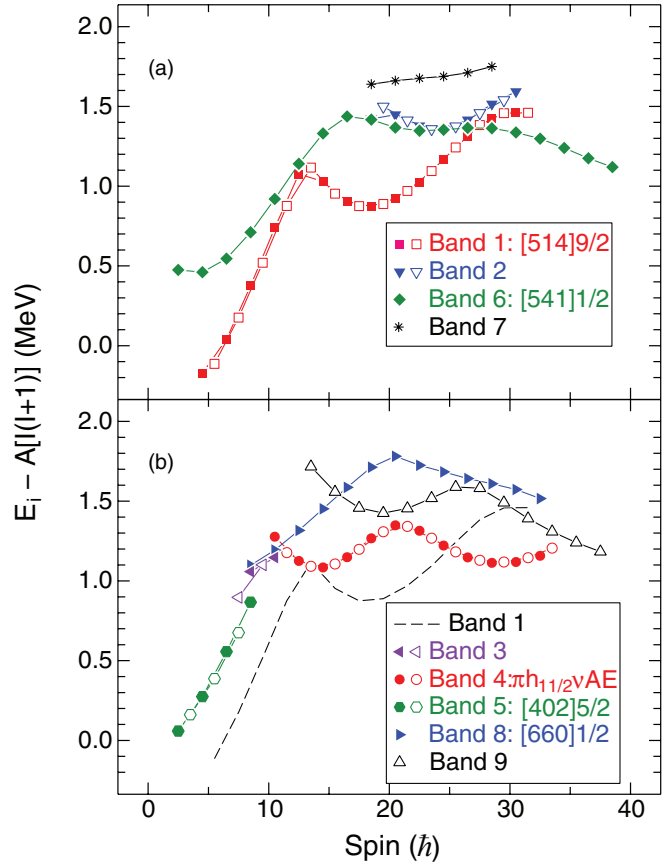

FIG. 3. (Color online) Excitation energies of the observed levels minus a rigid-rotor reference, where this reference was assumed to have a moment of inertia parameter $A = 0.007$ MeV. Positive (negative) signatures are represented with solid (open) symbols.

C. Band 3

A short sequence of levels strongly feeding band 1 through multiple transitions is labeled as band 3 in Fig. 1. These states were previously observed in Ref. [9] and were associated with the structure labeled band 4 in Fig. 1. Many of the γ rays can be seen in coincidence with the gates set in band 4, which are displayed in Fig. 2(c) and denoted with a plus (+) sign. Of the linking transitions between bands 3 and 1, where angular correlations could be measured, none exhibited a ratio consistent with a stretched electric quadrupole nature. Rather, the ratios had values typical of stretched and unstretched dipole transitions. It is, therefore, possible that band 3 has parity opposite to band 1, and it was tentatively assigned positive parity.

The decay path of band 3 is complex and several discrepancies are found between Fig. 1 and the level scheme in Ref. [9]. For example, no 107-keV line was observed in the present study, and the 176-keV transition was found to be in coincidence with both 192-keV γ rays (Ref. [9] indicated that the 176-keV line was in a parallel decay path with one of the 192-keV transitions). In addition, these levels were separated from band 4 as they create a significant discontinuity of the band structure if they are associated with the bottom of band 4. In the interpretation of Fig. 1, bands 3 and 4 resemble the structures labeled as bands 3 and 2, respectively, in a publication of high-spin states in ^{167}Re [18].

D. Band 4

The strongly coupled structure labeled band 4 in Fig. 1 was previously identified in Ref. [9] up to spin 39/2. An increase of one unit of $\hbar$ was assigned to the states in comparison to the previous level scheme. This is based on the observation of the 192- and 384-keV transitions from the 23/2 state in band 4 to the 21/2 and 19/2 levels, respectively, in band 3 and that both 192-keV transitions have an angular-correlation ratio consistent with $\Delta I = 1$. In addition, the present spin assignment suggests that band 4 lies at lower energies than band 1 above spin 49/2, which is consistent with the observed relative intensities between the bands. The structure was extended to a spin of 67/2, and a supporting spectrum is displayed in Fig. 2(c). Although direct evidence for the 61-keV transition from the 23/2 to the 21/2 state is lacking, band 4 is clearly in coincidence with the 324- and 691-keV

transitions depopulating the level. The 61-keV line is likely an $M1$ transition and, therefore, has a large internal-conversion coefficient that leads to the difficulty of observing the line in a γ-ray spectrum. Positive parity was assigned to this sequence based on the configuration assignment discussed in Sec. V D.

E. Band 5

A new, short sequence was identified and labeled as band 5 in Fig. 1. Some of the transitions can be seen in the spectrum from band 4 in Fig. 2(c) owing to the feeding 191-, 367-, and 691-keV transitions. These peaks are denoted with a hexagon in Fig. 2(c). No reliable angular-correlation ratios could be extracted for the linking transitions, and the spin and parity assignments must be considered as tentative as a result. However, the proposed assignment suggests a $5/2$ bandhead state that is 119 keV above the proposed ground state. Because the only known state below this 119-keV level is the $9/2^-$ ground state, an $M2$ transition would be required for γ decay. A Weisskopf estimate of approximately 40 μs can be made for the partial half-life of the state based on such a transition. Such a γ ray would not be observed in the current prompt spectroscopy data. The positive-parity assignment is based on the configuration assignment discussed in Sec. V E.

F. Band 6

Band 6 in Fig. 1 was previously seen in Ref. [9] up to $41/2$, but no connecting transitions were found for this decoupled sequence. In the present experiment, three weak linking transitions (497, 634, and 887 keV) were observed feeding into band 1 such that the relative excitation energy of band 6 has now been established. The 887-keV line has an angular-correlation ratio that is consistent with a stretched-$E2$ transition, making the 497- and 634-keV lines unstretched. This structure was extended to $77/2$, the highest spin state observed in this nucleus. The negative-parity assignment is based on the configuration assignment for band 6, which is addressed in Sec. V F. An example spectrum is provided in Fig. 4(a). The peaks denoted with a cross ($\times$) in the spectrum result from a short sequence that is observed feeding into band 6 at high spin, and has been labeled band 6a in Fig. 1.

The 320-keV feedout transition from the $5/2$ state seen in Ref. [9] was confirmed, and a 355-keV line was found decaying out of the $9/2$ state. Both of these transitions have angular-correlation ratios consistent with a dipole character (see Table I). Neither of these transitions feeds states that were identified in the other decay sequences. At 216 keV, the $3/2$ level could γ decay to the $(5/2)$ state in band 5; however, the resultant 97-keV line cannot be observed in the coincidence spectra. If the $3/2$ level has positive parity, the 97-keV transition would be $M1$ in nature and, thus, be highly converted, making the observation of the γ ray difficult. This suggests that the $3/2$ state could possibly be associated with positive parity.

G. Band 7

A new decoupled sequence has been found feeding into band 6. Coincident transitions of band 7 are denoted with an asterisk (*) in the spectrum for band 6 [Fig. 4(a)]. Both of the linking transitions were found to be of $E2$ character from the angular-correlation analysis (Table I); therefore, the relative

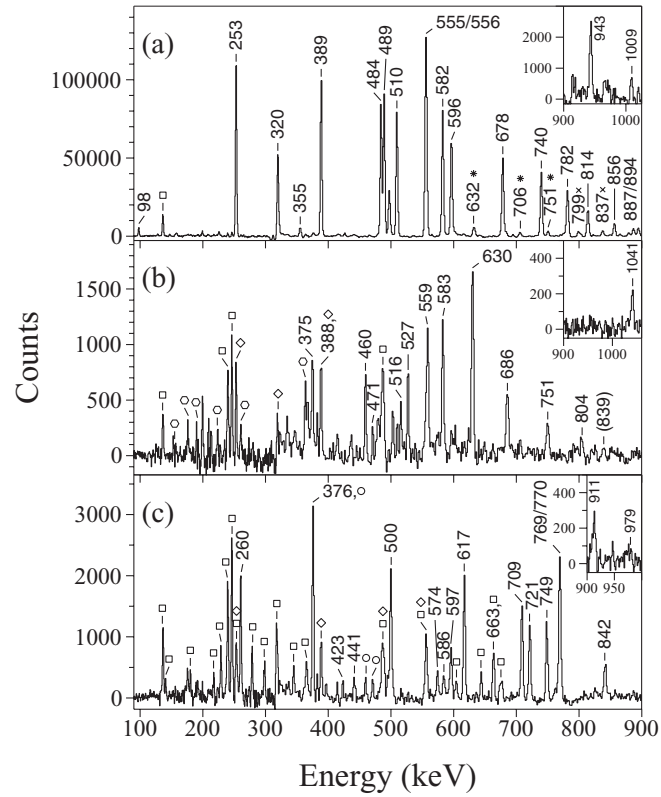

FIG. 4. (a) Spectrum of band 6 resulting from a sum of gates on all $E2$ transitions in the structure. The inset is a continuation of the main spectrum. Peaks marked with squares, crosses, and asterisks are from bands 1, 6a, and 7, respectively. (b) Spectrum of band 8 produced by summing all triple gates placed on inband $E2$ transitions. Peaks labeled with squares, hexagons, and diamonds result from bands 1, 5, and 6, respectively. (c) Spectrum of band 9 created in a manner similar to the spectra in panels (a) and (b). Peaks denoted with squares, diamonds, and circles are from bands 1, 6, and 8, respectively.

spins of band 7 have been verified and it must have the same (negative) parity as band 6.

H. Band 8

Another new decoupled structure was observed feeding into both bands 1 and 6. An example spectrum of this sequence is provided in Fig. 4(b) and it is labeled band 8 in Fig. 1. The angular-correlation-ratio analysis of the two linking transitions from the lowest observed level in band 8 indicates that both have dipole nature even though one (1041 keV) feeds the $15/2$ state in band 1, while the other (388 keV) feeds the $17/2$ level in band 6. It has been assumed that the higher-energy γ ray is of stretched dipole character, while the other is unstretched. This leads to the $17/2$ spin assignment for the lowest state observed in band 8. The positive parity is proposed based on the configuration assignment (see Sec. V H). This structure was extended to a spin of $61/2$ (tentatively $65/2$). In addition, there is an interaction with a nearly degenerate $25/2$ state. One may also observe in the spectrum of Fig. 4(b) that several peaks are denoted with a hexagon, indicating that coincidence between bands 8 and 5 is likely; however, no linking transitions could be readily identified between the two sequences.

I. Band 9

Finally, a new decoupled sequence whose decay is fragmented through many transitions into bands 1, 6, and 8 was observed. The structure is labeled band 9 in Fig. 1, and the coincidence with the three other bands can be observed in the spectrum of Fig. 4(c). Unfortunately, the linking transitions were too weak to obtain angular-correlation ratios. However, because the linking transitions from the lowest state in band 9 feed states with spins 25/2 and 27/2, a tentative spin assignment of 27/2 is proposed. Once again, the parity assignment is based on the proposed configuration, for which the reader is referred to Sec. V I.

IV. LEVEL SCHEME FOR ^{170}Re

Only a few studies of the odd-odd nucleus ^{170}Re can be found in the literature. A tentative (5^+) assignment for the ground state was suggested by Schmidt-Ott *et al.* [16] from α-decay spectroscopy. This study also reported five excited states. Four low-energy levels were observed in the electron-capture decay analysis of ^{170}Os [19]. Wang *et al.* [10] associated a rotational band with ^{170}Re through the observation of coincident rhenium x rays and a two-point excitation function.

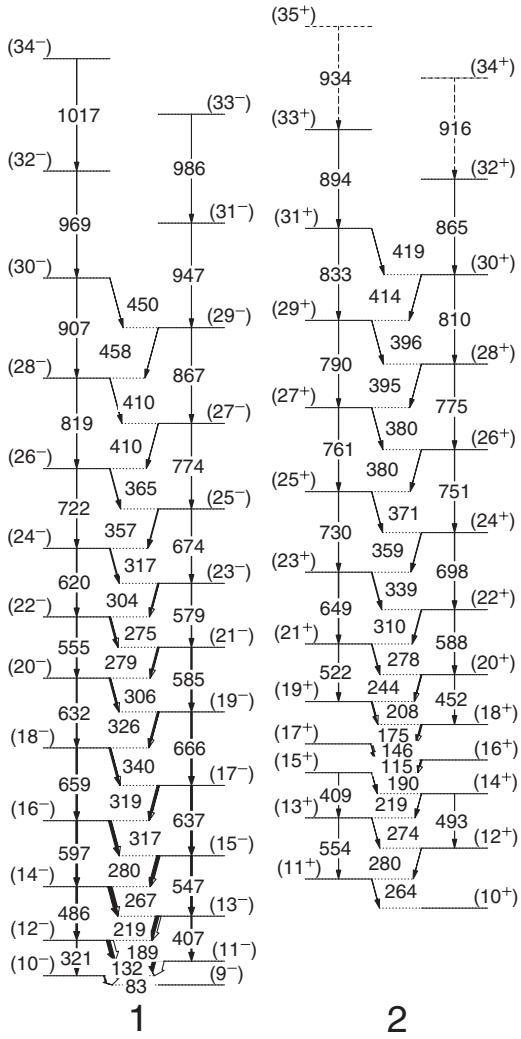

FIG. 5. Level scheme for ^{170}Re. All spins and parities must be considered tentative (see text for details).

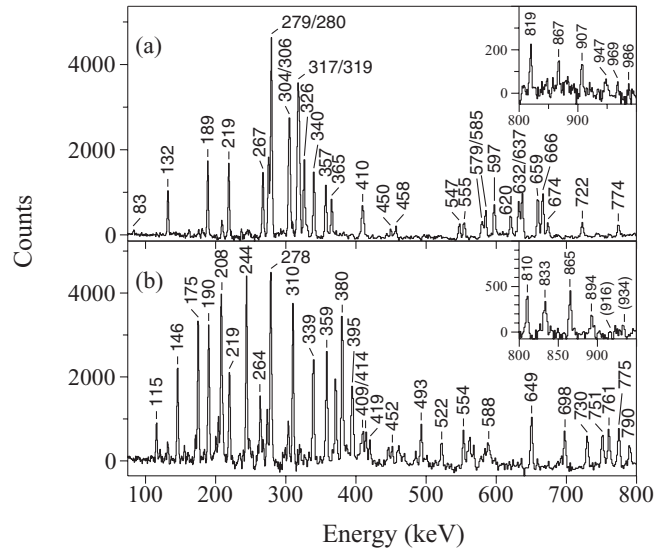

FIG. 6. (a) Spectrum of band 1 in ^{170}Re resulting from a sum of spectra where coincidence between any two dipole transitions between the spin 10 and 16 states along with any dipole γ ray between the 19 and 28 states was required. The inset is a continuation of the main spectrum. (b) Spectrum of band 2 where any three dipole transitions between levels 16 and 28 were in coincidence. Once again, the inset is a continuation of the main spectrum.

The aforementioned band was also observed in the present experiment and was confirmed to be in coincidence with rhenium x rays. In addition, the same sequence was found in a similar experiment, where the target was changed to ^{120}Sn and the ^{55}Mn beam energy was reduced to 253 MeV to enhance the $4n$ channel leading to states in ^{171}Re [20]. The fact that the band was seen in both experiments indicates that it is likely to be associated with ^{170}Re, where it was produced in the $3n$ channel of this experiment, and in the $5n$ channel of the short experiment using the ^{120}Sn target. This structure is presented in Fig. 5 as band 1, where it was extended from a previous maximum spin of 22 to 34. An example spectrum is provided in Fig. 6(a). No linking transitions to the previously identified low-spin states were found; therefore, the exact excitation energy of the band is unknown. The same tentative spin/parity assignments suggested in Ref. [10] are adopted based on systematics of neighboring nuclei and the proposed configuration of the sequence.

A second sequence was observed in both experiments mentioned above and is in coincidence with rhenium x rays. The intensity of this band changed between the two experiments mentioned above in a similar manner as the structure previously assigned to ^{170}Re; therefore, band 2 in Fig. 5 has been tentatively assigned to this odd-odd nucleus as well. Very few structures resembling this band are observed in nearby nuclei, thus, systematics could not be used to propose spins. Instead, spins were tentatively assigned based on the proposed configuration assignment to render the observed alignment values consistent with the expected initial alignment

TABLE II. γ-ray energies and intensities in ^{170}Re.

I^{π} [a]	E_{level} (keV)	E_{γ} (keV)[b]	I_{γ} [c]	Angular correlation ratio
		Band 1: $\pi h_{11/2}\nu i_{13/2}$ $\alpha = 0$		
(10^-)	X + 83.2	83.2	∼35[d]	
(12^-)	X + 403.8	320.6	∼19[e]	
		188.6	∼105[e]	0.59(2)
(14^-)	X + 889.6	485.8	46(4)	
		267.4	90(5)	0.64(2)
(16^-)	X + 1486.8	597.2	47(3)	0.72(3)
		317.4	67(4)	0.65(3)[f]
(18^-)	X + 2146.3	659.5	40(3)	0.94(4)
		340.1	45(3)	0.64(2)
(20^-)	X + 2778.2	631.9	27(2)	1.05(5)
		305.9	38(5)	0.62(3)[f]
(22^-)	X + 3332.8	554.6	23(2)	0.78(6)
		275.4	34(2)	0.57(2)
(24^-)	X + 3953.2	620.4	20(2)	1.03(8)
		316.5	22(3)	0.65(3)[f]
(26^-)	X + 4675.4	722.2	10(1)	
		364.9	16(1)	0.68(4)
(28^-)	X + 5494.7	819.3	8.0(6)	
		409.8	7.1(6)	
(30^-)	X + 6402.0	907.3	2.9(3)	
		449.9	<2	
(32^-)	X + 7371	969	<2	
(34^-)	X + 8388	1017	<2	
		Band 1: $\pi h_{11/2}\nu i_{13/2}$ $\alpha = 1$		
(9^-)	X			
(11^-)	X + 215.1	131.9	∼95[d]	0.59(3)
(13^-)	X + 622.2	407.1	∼30[e]	
		218.5	≡100(4)	0.62(2)
(15^-)	X + 1169.4	547.2	49(4)	0.99(8)
		279.7	76(8)	0.67(3)[f]
(17^-)	X + 1806.3	636.9	52(3)	0.98(4)
		319.4	56(6)	0.65(3)[f]
(19^-)	X + 2472.4	666.1	42(3)	0.99(8)
		326.1	43(3)	0.64(2)
(21^-)	X + 3057.4	585.0	36(3)	
		279.1	37(4)	0.67(3)[f]
(23^-)	X + 3636.7	579.3	14(1)	1.02(8)
		303.8	30(3)	0.62(3)[f]
(25^-)	X + 4310.6	673.9	10.0(7)	
		357.3	19(1)	0.61(3)
(27^-)	X + 5085.0	774.4	7.9(5)	
		409.5	9.5(8)	
(29^-)	X + 5952.3	867.3	5.0(3)	
		457.5	4.4(2)	
(31^-)	X + 6899	947	<2	
(33^-)	X + 7885	986	<2	
		Band 2: $\pi h_{11/2}\nu E$ $\alpha = 0$		
(10^+)	Y			
(12^+)	Y + 543.3	279.5	2.9(3)[d]	
(14^+)	Y + 1036.4	493.1	3.5(3)[e]	
		219.0	4.7(4)[e]	
(16^+)	Y + 1341.7	115.2	8.0(6)	
(18^+)	Y + 1662.7	175.3	20(1)	
(20^+)	Y + 2114.4	451.7	5.7(4)	
		244.0	17(1)	
(22^+)	Y + 2702.8	588.4	9.8(7)	
		310.2	16(1)	
(24^+)	Y + 3400.4	697.6	9.9(7)	
		358.6	12(1)	
(26^+)	Y + 4151.7	751.3	7.8(6)	
		380.3	7.6(8)	
(28^+)	Y + 4926.5	774.8	6.1(4)	
		394.6	3.8(4)	
(30^+)	Y + 5736.2	809.7	2.9(2)	
		414.2	<2	
(32^+)	Y + 6601	865	<2	
(34^+)	(Y + 7517)	(916)	<2	
		Band 2: $\pi h_{11/2}\nu E$ $\alpha = 1$		
(11^+)	Y + 263.8	263.8	∼6[d]	
(13^+)	Y + 817.4	553.6	4.7(3)	
		274.1	2.9(2)	
(15^+)	Y + 1226.6	409.2	3.5(2)	
		190.1	4.4(3)	
(17^+)	Y + 1487.5	145.7	19(2)	
(19^+)	Y + 1870.4	207.6	19(2)	
(21^+)	Y + 2392.6	522.2	8.7(6)	
		278.3	14(1)	
(23^+)	Y + 3041.8	649.2	15(1)	
		339.0	17(1)	
(25^+)	Y + 3771.4	729.6	7.2(5)	
		370.9	4.8(5)	
(27^+)	Y + 4532.0	760.6	7.6(5)	
		380.4	4.8(5)	
(29^+)	Y + 5322.1	790.1	3.8(3)	
		395.5	2.9(3)	
(31^+)	Y + 6155	833	<2	
		419	<2	
(33^+)	Y + 7049	894	<2	
(35^+)	(Y + 7983)	(934)	<2	

[a]Spin and parity of the depopulated state.
[b]Uncertainties in γ-ray energy are 0.2 keV for most transitions, except for relatively weak transitions ($I_{\gamma} < 2$), where 0.5 keV uncertainties are appropriate.
[c]Relative intensity of the transition with respect to the intensity of the 218.5-keV transition.
[d]Estimated based on intensity balance.
[e]Estimated based on intensity balance and branching ratio.
[f]Unresolved doublet.

of the configuration. A spectrum is displayed in Fig. 6(b). In addition, a table of the level and γ-ray information for ^{170}Re is given in Table II.

V. DISCUSSION

To interpret the quasiparticle configurations associated with the bands in ^{169}Re, the alignments for all the bands are displayed as a function of rotational frequency in Fig. 7. Harris parameters of $\mathcal{J}_0 = 17\,\hbar^2/\text{MeV}$ and $\mathcal{J}_1 = 50\,\hbar^4/\text{MeV}^3$ were used to subtract a reference associated with the angular

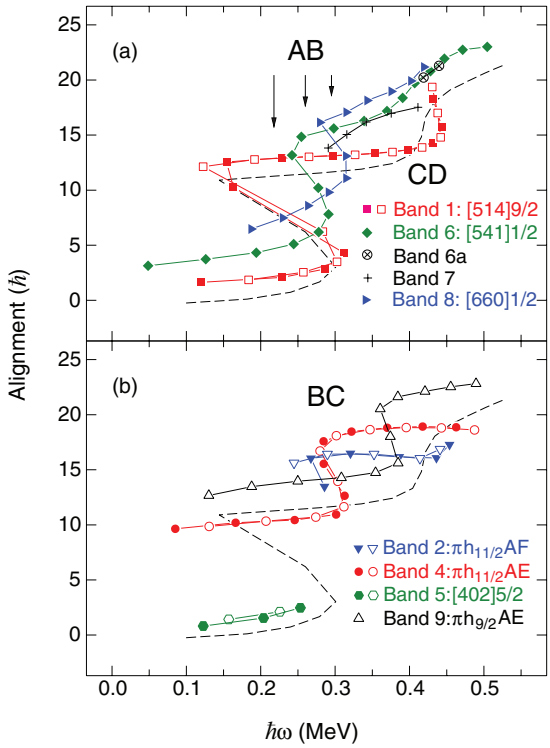

FIG. 7. (Color online) Alignments of the bands in ^{169}Re plotted versus the rotational energy $\hbar\omega$. Harris parameters of $\mathcal{J}_0 = 17\,\hbar^2/\mathrm{MeV}$ and $\mathcal{J}_1 = 50\,\hbar^4/\mathrm{MeV}^3$ were used to subtract the angular momentum of the rotating core. Observed crossings are designated in the figure. Solid (open) symbols denote the $\alpha = +1/2$ $(-1/2)$ sequences. The dashed line represents the alignment observed in the ground-state band in ^{168}W.

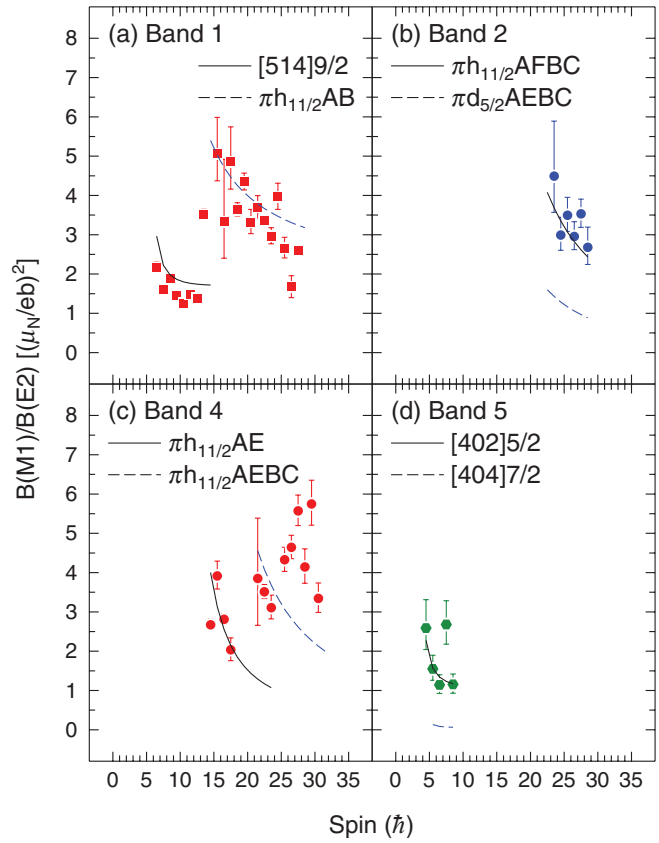

FIG. 8. (Color online) Experimental and theoretical $B(M1)/B(E2)$ ratios for bands 1, 2, 4, and 5 in ^{169}Re. Parameters for the theoretical calculations are discussed in the text and given in Table III.

momentum generated by the rotation of the even-even core nucleus ^{168}W. In addition, the ground-state band of ^{168}W [21] is given in Fig. 7 for reference. Several band crossings are seen in the alignment diagram; therefore, cranked shell model (CSM) [22] calculations were performed to associate these crossings with likely quasiparticle alignments. A quadrupole deformation of $\beta_2 = 0.19$ was assumed based on calculations from Ref. [23], and a fixed neutron pairing energy of 1.28 MeV was used. From these calculations, the lowest pair of $i_{13/2}$ quasineutrons (AB) is predicted to align at a frequency of 0.23 MeV, the second (BC) at 0.35 MeV, the third (AD) at 0.37 MeV, and the fourth one (CD) at 0.53 MeV, while the first proton crossing (based on $h_{11/2}$ quasiprotons E_pF_p) is computed to occur at 0.51 MeV. In addition, $B(M1)/B(E2)$ transition strength ratios were determined and compared with theoretical estimates in Fig. 8 for the strongly coupled bands 1, 2, 4, and 5.

A. Band 1

This structure was previously associated with the [514]9/2 quasiproton configuration originating from the $h_{11/2}$ shell [9]. Its initial alignment is approximately 1.5 $\hbar$, as seen in Fig. 7(a), which is consistent with, although slightly lower than, the CSM estimate of 2.6 $\hbar$. The lesser value may be an indication of mixing with the $K = 11/2$ orbital. The first crossing at 0.23 MeV can be confidently identified with the AB alignment as it matches the crossing frequency and alignment gain predicted in the CSM as well as the observed AB crossing in the neighboring even-even nucleus ^{168}W. A satisfactory agreement is also found between the experimental and theoretical $B(M1)/B(E2)$ ratios seen in Fig. 8(a). The predicted ratios were calculated based on the geometrical approximation for $B(M1)$ strengths [24] and the rotational form for the $B(E2)$ reduced probabilities [25]. Parameters used in the calculation of the theoretical $B(M1)/B(E2)$ ratios are given in Table III, along with $g_R = Z/A = 0.444$ and $Q_0 = 5.1$ eb (assuming $\beta_2 = 0.19$). The experimental values were determined by gating above the state of interest and the branching ratio was measured from the corresponding spectra. Thus, the branching ratio may be slightly different from that calculated with the reported intensities in Table I. As a result of the comparisons between computed and observed $B(M1)/B(E2)$ ratios and alignments, the [514]9/2 configuration is confirmed for band 1.

At higher frequencies, the beginning of a second crossing can be observed in Fig. 7(a) near 0.44 MeV, similar to that seen in the ground-state band of ^{168}W. Although this is at a lower frequency than the CSM-predicted value of 0.53 MeV, this crossing is associated with the CD alignment as the $h_{11/2}$ quasiproton crossing is Pauli blocked in a band where the

TABLE III. Parameters used in calculating the theoretical $B(M1)/B(E2)$ values shown in Fig. 8.

Configuration	g_Ω	i_x ($\hbar$)
$\pi h_{11/2}[514]9/2$	1.30	1.4
$\pi d_{5/2}[402]5/2$	1.57	0.0
$\pi g_{7/2}[404]7/2$	0.62	0.0
$\nu i_{13/2}$ AB	−0.3	11.0
$\nu i_{13/2}$ BC	−0.3	8.0
$\nu i_{13/2}$ A	−0.3	6.0
$\nu h_{9/2}$ E, F	−0.32	2.0

[514]9/2 orbital is occupied. The lower crossing frequency may be the result of reduced neutron pairing correlations following the AB crossing. This assignment is consistent with the interpretation of the crossing found near 0.42 MeV in the ground-state band in ^{168}W resulting from the alignment of the CD and possibly EF quasineutrons [21].

B. Band 2

This new sequence is likely based on a five-quasiparticle configuration as it is observed at a much higher excitation energy than the AB crossing in band 1. The alignment profile of band 2, in Fig. 7(b), indicates that this structure may be observed just after completion of the same crossing found in band 4. As discussed in Sec. V D, this is the BC crossing, which suggests that the A quasineutron is involved with the initial configuration of band 2. Both the AE and the AF configurations were observed in ^{168}W [21], and it is likely that band 2 is based on one of these quasineutron pairs coupled to a quasiproton. The $\pi h_{11/2}\nu AE$ configuration has been assigned to band 4 (see Sec. V D); therefore, the $\pi h_{11/2}\nu AFBC$ and $\pi d_{5/2}\nu AEBC$ configurations are most likely associated with band 2. Both possibilities would have slightly less alignment above the BC crossing than band 4 ($\pi h_{11/2}\nu AE$) as the AF configuration was found to have $\sim$1.5 $\hbar$ less alignment than the AE one at high frequencies in ^{168}W, and the $d_{5/2}$ quasiproton has $\sim$1 $\hbar$ less alignment than the $\pi h_{11/2}$ quasiproton. Thus, the theoretical $B(M1)/B(E2)$ ratios for these two configurations were compared with the experimental values in Fig. 8(b). Once again, parameters for the different configurations are given in Table III. Good agreement is found between the experimental ratios and the predicted values for the $\pi h_{11/2}\nu AFBC$ configuration; therefore, a tentative assignment with this configuration is proposed for band 2.

C. Band 3

As there are only a few states and γ rays seen in this band, there is insufficient information to assign a configuration for this sequence.

D. Band 4

The fact that band 4 is observed at $\sim$2100 keV and that it has approximately 10 $\hbar$ of initial alignment strongly suggests that it is associated with a three- quasiparticle sequence.

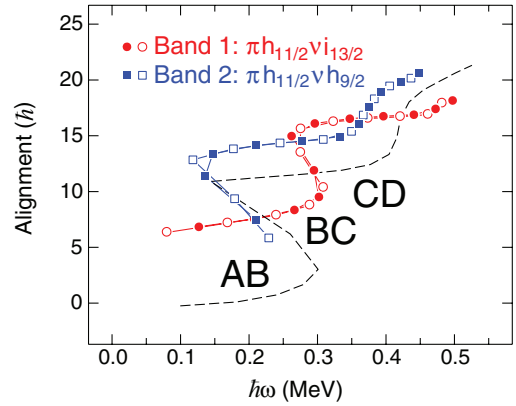

FIG. 9. (Color online) Alignments of the bands in ^{170}Re plotted versus the rotational energy $\hbar\omega$. Harris parameters of $\mathcal{J}_0 = 17\,\hbar^2/\text{MeV}$ and $\mathcal{J}_1 = 50\,\hbar^4/\text{MeV}^3$ were used to subtract the angular momentum of the rotating core. Observed crossings are designated in the figure. Solid (open) symbols denote the $\alpha = +1/2$ $(-1/2)$ sequences. The dashed line represents the alignment observed in the ground-state band in ^{168}W.

The AB crossing is clearly blocked, but a crossing is found in Fig. 7(b) at 0.30 MeV, which is near the predicted BC crossing frequency and is consistent with the observation of this crossing frequency in the $\pi h_{11/2}\nu i_{13/2}$ band in ^{170}Re at 0.29 MeV (see Fig. 9). This suggests that the A quasineutron is involved in the initial configuration. As this quasineutron is normally associated with 6 $\hbar$ of alignment, the other two quasiparticles must account for approximately 4 $\hbar$. In many nearby nuclei, a structure interpreted as the $\pi h_{11/2}\nu AE$ configuration is observed to strongly mix with either the $\pi d_{5/2}$ or the $\pi g_{7/2}$ configurations during or just after the AB crossing [26–28]. The E label refers to the lowest negative-parity orbital near the Fermi surface, and from ^{169}W [29], this orbital has approximately 2 $\hbar$ of initial alignment. Therefore, the individual quasiparticle alignments of the $\pi h_{11/2}\nu AE$ configuration sum to a value close to that of band 4. In addition, the predicted $B(M1)/B(E2)$ ratios for this configuration agree with the experimental values, as seen in Fig. 8(c). Thus, band 4 is interpreted as the $\pi h_{11/2}\nu AE$ configuration. It should be noted that band 4 does not undergo the CD alignment at high frequencies, which is consistent with the proposed assignment.

E. Band 5

This short sequence was not extended sufficiently high to observe a band crossing. However, the fact that it is strongly coupled and has nearly zero initial alignment [see Fig. 7(b)] suggests that it is based on either the [402]5/2 or the [404]7/2 quasiproton configuration. These two orbitals have very different g_Ω values (see Table III) which lead to distinguishing $B(M1)/B(E2)$ ratios. The band was too weak to extract branching ratios from gates above the states of interest; therefore, branching ratios were determined from the observed intensities. A comparison of the experimental ratios with the calculated values of the [402]5/2 and [404]7/2 configurations are shown in Fig. 8(d). The experimental ratios

clearly favor the [402]5/2 configuration, and thus band 5 is associated with this quasiproton.

F. Band 6

This decoupled sequence was previously assigned as the [541]1/2 structure in Ref. [9]. As seen in Fig. 7(a), the initial alignment of 3 $\hbar$ is consistent with this assignment. In addition, the first crossing is delayed in this band until a frequency of 0.27 MeV. The delay of the AB crossing is a characteristic of the [541]1/2 orbital [30]. A larger deformation for the sequence based on the [541]1/2 orbital compared with the other orbitals is thought to cause the delayed crossing. Surprisingly, a second crossing is found at 0.43 MeV, which is below the frequency where the second crossing (CD) in band 1 and the ground-state band in ^{168}W are observed. If the second crossing in band 6 is indeed the CD alignment, one might expect it to be delayed as well. Therefore, this alignment does not seem likely for the second crossing in band 6. Perhaps, the alignment gain is associated with the mixing of another band, such as band 6a that is seen in Fig. 1, which is observed in the same frequency range as the second crossing.

G. Band 7

Assigning a configuration for band 7 is quite challenging with the limited information that can be deduced about the sequence. Based upon its excitation energy, it could either be associated with a three- or five-quasiparticle band. From the alignment plot of Fig. 7(a), it could be a band following either the AB or BC crossing as it has an initial alignment of approximately 13 $\hbar$ near 0.3 MeV. Because it is decoupled, the constituent quasiparticles are likely of low K values. Therefore, the [541]1/2, [411]1/2, and [660]1/2 quasiprotons are possibly involved. The spin assignment forbids an assignment of the signature partner of the [541]1/2 band. Band 8 has been assigned the [660]1/2 configuration (see below); therefore, the [411]1/2 quasiproton may be the best candidate. Band 7 has been determined to have negative parity, such that a negative-parity quasineutron may be involved. With these considerations, a possible configuration for band 7 would be π[411]1/2$\nu AEBC$, but this assignment must be regarded as a tentative.

H. Band 8

Band 8 has an initial alignment of approximately 6 $\hbar$ and displays a crossing near 0.30 MeV [see Fig. 7(b)]. The initial alignment is somewhat low for a three-quasiparticle structure, but is consistent with that expected for the $i_{13/2}$[660]1/2 quasiproton. This assignment suggests that the crossing is from the AB alignment, which is significantly delayed with respect to that seen in band 1. A large delay in the AB crossing is also consistent with the [660]1/2 configuration as this trait has been observed in several nearby nuclei [7,31]. Similar to the [541]1/2 band, the delay is likely the result from a larger deformation associated with this sequence. Therefore, band 8 is assigned the [660]1/2 configuration. The [660]1/2 band is particularly interesting in this region as collective wobbling bands have been observed based on this configuration. A discussion of the search for wobbling is given in Sec. VI.

I. Band 9

The initial alignment of band 9, seen in Fig. 7(b), is approximately 2–3 $\hbar$ larger than that of band 4, which was assigned the $\pi h_{11/2}\nu AE$ configuration. In addition, a crossing is observed at 0.37 MeV which lies between the expected BC and CD alignments. A configuration assignment of $\pi h_{9/2}\nu AE$ for band 9 can best describe these characteristics. This configuration should have a larger alignment of $\sim$2$\hbar$ compared with the $\pi h_{11/2}\nu AE$ configuration, and a delayed BC crossing may be expected as a result of the likely larger deformation driven by the $h_{9/2}$ quasiproton. Based on these results, band 9 is tentatively assigned the $\pi h_{9/2}\nu AE$ configuration.

J. ^{170}Re: Bands 1 and 2

An alignment plot for the two bands in ^{170}Re is given in Fig. 9, where the same Harris parameters were used as in Fig. 7, and the ground-state band in ^{168}W is also given. Band 1 has an initial alignment of $\sim$6 $\hbar$ and the AB crossing is clearly blocked. However, the BC alignment is observed at 0.29 MeV, which is near the CSM predicted value. These facts indicate the A ($i_{13/2}$) quasineutron is involved with the configuration of band 1. Because the $h_{11/2}$ quasiproton was found to be yrast at lower spins in ^{169}Re, it is likely that band 1 has the $\pi h_{11/2}\nu i_{13/2}$ configuration. Indeed, the experimental $B(M1)/B(E2)$ ratios agree well with the theoretical values (where the same parameters in Table III were used) for this configuration, as shown in Fig. 10(a). Thus, this assignment of the $\pi h_{11/2}\nu i_{13/2}$ configuration agrees with that proposed in Ref. [10].

In Fig. 9, one may observe that band 2 closely tracks the ground-state band of ^{168}W. The fact that the AB alignment is seen implies that the $i_{13/2}$ quasineutron is not involved in the initial configuration of band 2. Instead, it is likely that the E quasineutron (from the $h_{9/2}$ shell) couples with the favored $h_{11/2}$ quasiproton to form this band. In addition, the theoretical $B(M1)/B(E2)$ ratios for the $\pi h_{11/2}\nu h_{9/2}$ configuration (following the AB crossing) are in agreement with the experimental ratios [Fig. 10(b)]. With this assignment, the spins of band 2 were adjusted to produce an alignment that is approximately 3 $\hbar$ larger than that of the ground-state band in ^{168}W. Clearly, this spin assignment must be regarded as tentative. At a higher frequency of 0.37 MeV, another crossing is observed in band 2. Although this occurs at a lower frequency than the CD alignment found in ^{168}W, it is likely that this crossing can be associated with the same pair of $i_{13/2}$ quasineutrons.

VI. SEARCH FOR THE WOBBLING STRUCTURE

As discussed previously, there is a predicted gap at $N = 94$ that may stabilize a nuclear shape associated with significant triaxial deformation [8]. In order for this gap to form, the

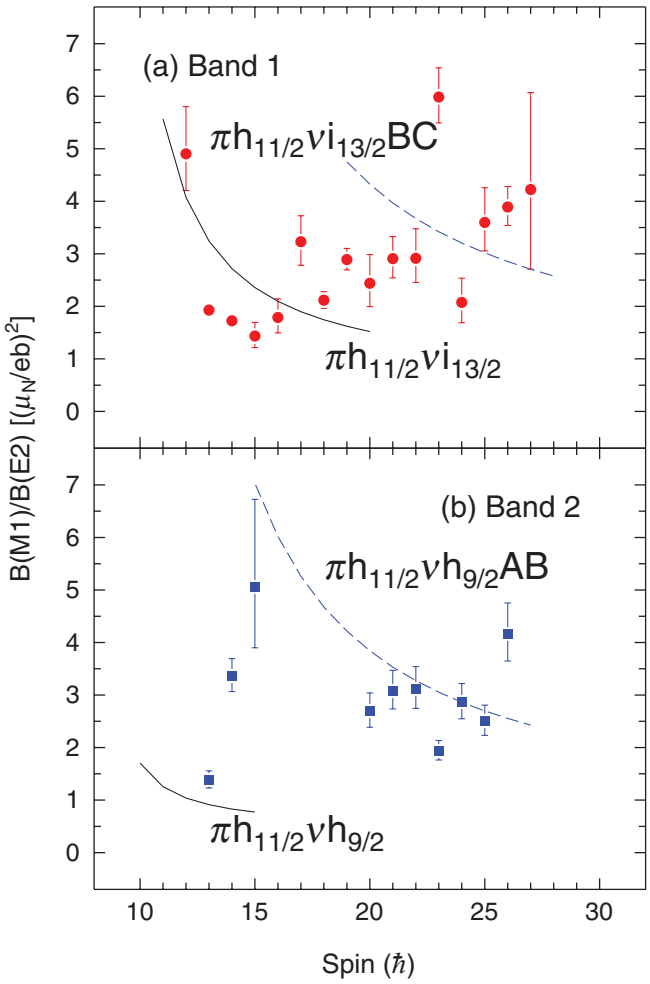

FIG. 10. (Color online) Experimental and theoretical $B(M1)/B(E2)$ ratios for bands in ^{170}Re. Parameters for the theoretical calculations are discussed in the text.

nuclear shape must also have a large quadrupole deformation, which naturally occurs with the occupation of the $\pi i_{13/2}$ orbital. For this reason, every wobbling excitation observed in this region has been based on a $\pi i_{13/2}$ sequence. With the new observation of the $\pi i_{13/2}$ band in ^{169}Re$_{94}$, an extensive search was conducted for a possible candidate band associated with wobbling that would feed into band 8. One of the principle characteristics of a wobbling band is that the alignment, dynamic moment of inertia, and quadrupole moment should be nearly identical to that of the $\pi i_{13/2}$ sequence because the wobbling band is based on the same configuration. The only difference is that the total angular momentum vector lies further off the body-fixed axes. In addition, the wobbling band should strongly feed the $\pi i_{13/2}$ structure through a number of $\Delta I = 1$ transitions.

A search was conducted using a number of coincidence gates with energy spacings that were similar to those in the $\pi i_{13/2}$ band below, above, and through the AB crossing. Similar energy spacings between proposed band members were used because a band with similar alignment and dynamic moment of inertia would be expected to exhibit such a property. Despite a thorough search, no signal consistent with a wobbling sequence could be identified. This does not necessarily imply that ^{169}Re cannot support the wobbling mode, but rather that such an excitation is below the present detection limits. In fact, the $\pi i_{13/2}$ band in ^{169}Re has a relative intensity that is approximately 10 times weaker than $\pi i_{13/2}$ bands where wobbling has been observed. This may explain why the wobbling mode could not be seen in ^{169}Re.

Figure 11 displays the excitation energies (minus a rigid-rotor reference) of the $\pi i_{13/2}$ (strongly deformed), $\pi h_{9/2}$ (intermediately deformed), and the favored signature of the $\pi h_{11/2}$ (normal deformed) bands near ^{169}Re. From this plot, it is clear that the $\pi i_{13/2}$ configuration lies high in energy for the lutetium, tantalum, and rhenium isotopes, while it lies relatively low in energy for iridium. However, one may note that the $\pi i_{13/2}$ sequence lies significantly higher with respect to the two other excitations in ^{169}Re than that found in the other nuclei of Fig. 11. This clearly accounts for the weak population of the $\pi i_{13/2}$ band in comparison to ^{163,165,167}Lu and ^{167}Ta, where wobbling has been found, making it difficult to identify a wobbling structure in ^{169}Re if one exists.

VII. RESIDUAL INTERACTIONS IN THE $\pi h_{9/2}\nu i_{13/2}$ AND $\pi i_{13/2}\nu i_{13/2}$ BANDS

Figure 11 not only provides insight into why a wobbling band could not be observed in ^{169}Re, it also raises questions about the doubly decoupled $\pi h_{9/2}\nu i_{13/2}$ and $\pi i_{13/2}\nu i_{13/2}$ bands. The $\pi i_{13/2}\nu i_{13/2}$ configuration is rarely seen in this region, with the only reported cases in ^{164}Lu [32] and ^{176}Ir [33], and the $\pi h_{9/2}\nu i_{13/2}$ structures are normally higher lying in energy than expected. For the latter case, as seen in Fig. 11, the $\pi h_{9/2}$ band is at or near the yrast line; therefore, one would expect the neighboring $\pi h_{9/2}\nu i_{13/2}$ bands in odd-odd nuclei to be located near the yrast line as well. However, a systematic investigation of this configuration in the $A \approx 170$ region reveals that it is typically not yrast and, in some cases (as in ^{170}Re), it is not observed at all. In addition, although the $\pi i_{13/2}$ configuration is normally observed at high energies at low spin ($<$20), it does not lie far from the yrast line at higher spins, such that it is somewhat surprising that more $\pi i_{13/2}\nu i_{13/2}$ sequences have not yet been observed.

To investigate this phenomenon further, a systematic study of the additivity of Routhians was performed for the $\pi h_{11/2}\nu i_{13/2}$, $\pi h_{9/2}\nu i_{13/2}$, and $\pi i_{13/2}\nu i_{13/2}$ configurations in this same region of Fig. 11. The Routhian is defined as the energy of the states in the frame of reference of the rotating nuclei, and it is an additive quantity [22]. Within the CSM, the Routhian of a band from an odd-odd nucleus should simply be the sum of the Routhians from the quasiparticles as measured in the neighboring odd-A nuclei. Any differences are associated with effects not included in the mean field and are labeled as residual interactions [34]. The results of a systematic additivity study are displayed in Table IV. The average Routhian energies for the $h_{11/2}$, $h_{9/2}$, and $i_{13/2}$ quasiprotons were determined at a frequency of 0.25 MeV from the neighboring even-N nuclei, and the average Routhian

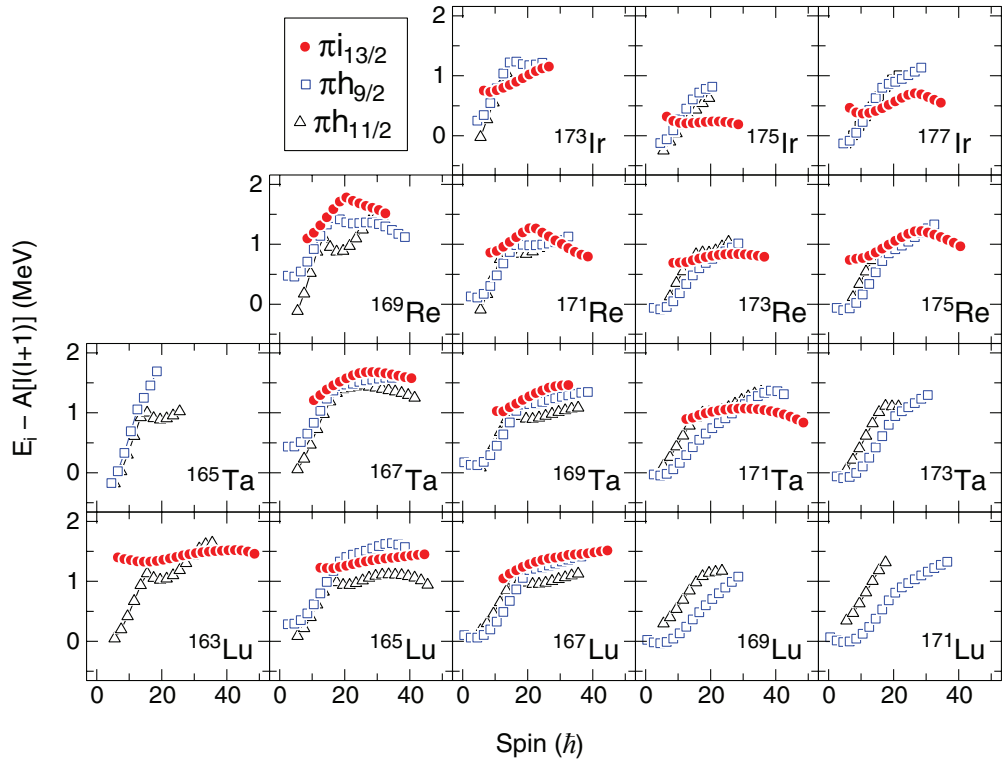

FIG. 11. (Color online) Relative excitation energy of states (minus a rigid-rotor reference) in the $\pi i_{13/2}$ (red circles), $\pi h_{9/2}$ (blue squares), and $\pi h_{11/2}$ (black triangles) bands in the nuclei specified. The moment of inertia parameter A was set to 0.007 MeV/$\hbar^2$.

energy for the $i_{13/2}$ quasineutron was found at the same frequency from the neighboring even-Z nuclei. These average values are listed under the columns of π and ν in Table IV. The sum of these values is given under the column denoted as Sum. If the configuration has been experimentally observed, its Routhian energy at $\hbar\omega = 0.25$ MeV is displayed under the Expt. column. The difference between the Expt. and Sum columns (Expt. − Sum) is then the residual interaction and is given in Table IV as Res. Int. It should be noted that the Routhian for the $\pi i_{13/2}\nu i_{13/2}$ band in ^{164}Lu was extrapolated down to a frequency of 0.25 MeV, and that the relative energies for the bands in ^{168}Lu and ^{172}Re are not known.

As can be seen in Table IV, the $\pi h_{11/2}\nu i_{13/2}$ configuration has a negative residual interaction in many of the isotopes, indicating that the coupling of these two quasiparticles leads to states that are lower in energy than expected. It is not surprising that this configuration is seen in all of the odd-odd nuclei given in the table and that it generally is the yrast configuration. However, the opposite effect is observed for the $\pi h_{9/2}\nu i_{13/2}$ structure, where the residual interaction is

TABLE IV. Calculated residual interactions for three bands in the $Z \approx 74$, $N \approx 96$ region. All Routhian energies (given in MeV) were determined at a frequency of 0.25 MeV with Harris parameters of $\mathcal{J}_0 = 28.5\hbar^2$/MeV and $\mathcal{J}_1 = 50\,\hbar^4$/MeV^3.

Nucleus	$\pi h_{11/2}\nu i_{13/2}$					$\pi h_{9/2}\nu i_{13/2}$					$\pi i_{13/2}\nu i_{13/2}$				
	π	ν	Sum	Expt.	Res. Int.	π	ν	Sum	Expt.	Res. Int.	π	ν	Sum	Expt.	Res. Int.
^{164}Lu	−0.20	−1.11	−1.31	−1.62	−0.31	−0.34	−1.11	−1.45	−1.33	+0.12	−0.02	−1.11	−1.13	∼−0.5	∼+0.6
^{166}Lu	−0.20	−1.08	−1.28	−1.22	+0.06	−0.49	−1.08	−1.57	−1.46	+0.11	−0.09	−1.08	−1.17	>−0.56	>+0.61
^{168}Lu	−0.17	−1.03	−1.20	−1.63	−0.43	−0.66	−1.03	−1.69	−1.95	−0.26	−0.11	−1.03	−1.14		
^{166}Ta	−0.21	−1.13	−1.34	−1.44	−0.10	−0.28	−1.13	−1.41	>−1.10	>+0.31	+0.15	−1.13	−0.98	>−1.10	
^{168}Ta	−0.14	−1.09	−1.23	−1.39	−0.16	−0.32	−1.09	−1.41	>−1.14	> +0.27	+0.07	−1.09	−1.02		
^{170}Ta	−0.19	−0.99	−1.18	−1.21	−0.03	−0.67	−0.99	−1.66	−1.51	+0.15	−0.23	−0.99	−1.22	>−1.07	>+0.15
^{172}Ta	−0.22	−0.88	−1.10	−0.80	+0.30	−0.85	−0.88	−1.73	−1.36	+0.37	−0.32	−0.88	−1.20	>−0.72	>+0.48
^{170}Re	−0.11	−1.00	−1.11	−1.13	−0.02	−0.26	−1.00	−1.26	>−1.13	> +0.13	0.00	−1.00	−1.00		
^{172}Re	−0.22	−1.06	−1.28	−1.16	+0.12	−0.64	−1.06	−1.70	−1.51	+0.19	−0.36	−1.06	−1.42		
^{174}Re	−0.30	−0.86	−1.16	−0.95	+0.21	−0.79	−0.86	−1.65	−1.43	+0.22	−0.45	−0.86	−1.31	>−1.08	>+0.23
^{176}Ir	−0.61	−0.84	−1.45	−1.20	+0.25	−0.71	−0.84	−1.55	−1.67	−0.12	−0.95	−0.84	−1.79	−1.37	+0.42

typically positive, revealing that the configuration has been shifted higher in energy. The residual interaction is between 100 and 250 keV for most cases, which significantly shifts the configuration away from the yrast line. Only a few examples for the $\pi i_{13/2}\nu i_{13/2}$ band can be inspected, but in those cases, the residual interaction is positive with large values (above 400 keV). Thus, it appears that the high-j, low-K quasiprotons coupled with the $i_{13/2}$ quasineutron systematically create a repulsive force driving the band to higher energies. Why such a large residual interaction occurs for the $\pi h_{9/2}\nu i_{13/2}$ and $\pi i_{13/2}\nu i_{13/2}$ structures is unknown and requires further theoretical investigation.

VIII. SUMMARY

Nine decay sequences are now known in ^{169}Re, including the $\pi i_{13/2}$ band that is the basis for wobbling structures in nearby nuclei. Wobbling could not be identified in this nucleus as the $\pi i_{13/2}$ band was relatively weakly populated owing to it lying high in energy relative to the yrast structures. Configurations for eight of the sequences were proposed based on their alignment characteristics and $B(M1)/B(E2)$ ratios. In addition, the previously known structure in ^{170}Re was extended to higher spin and a new sequence was tentatively assigned to this odd-odd system. An analysis of the residual interactions of the $\pi h_{9/2}\nu i_{13/2}$ and $\pi i_{13/2}\nu i_{13/2}$ configurations suggests that these two structures are typically pushed higher in energy, which explains why they are either not seen or are weaker than expected. However, a more complete understanding requires further theoretical work.

ACKNOWLEDGMENTS

The authors thank the ANL operations staff at Gammasphere and gratefully acknowledge the efforts of J. P. Greene for target preparation. We thank D. C. Radford and H. Q. Jin for their software support. This work is funded by the National Science Foundation under Grants No. PHY-1203100 (USNA), No. PHY-0754674 (FSU), and No. PHY10-68192 (ND), as well as by the US Department of Energy, Office of Nuclear Physics, under Contracts No. DE-AC02-06CH11357 (ANL), No. DE-FG02-94ER40848 (UML), No. DE-FG02-96ER40983 (UT), and No. DE-FG02-94ER40834 (UMCP).

[1] S. W. Ødegård *et al.*, Phys. Rev. Lett. **86**, 5866 (2001).
[2] G. Schönwaßer *et al.*, Phys. Lett. B **552**, 9 (2003).
[3] H. Amro *et al.*, Phys. Lett. B **553**, 197 (2003).
[4] P. Bringel *et al.*, Eur. Phys. J. A **24**, 167 (2005).
[5] N. S. Pattabiraman *et al.*, Phys. Lett. B **647**, 243 (2007).
[6] D. J. Hartley *et al.*, Phys. Rev. C **80**, 041304(R) (2009).
[7] D. J. Hartley *et al.*, Phys. Rev. C **83**, 064307 (2011).
[8] H. Schnack-Petersen *et al.*, Nucl. Phys. A **594**, 175 (1995).
[9] X. H. Zhou *et al.*, Eur. Phys. J. A **19**, 11 (2004).
[10] H. L. Wang *et al.*, Phys. Rev. C **70**, 064306 (2004).
[11] R. V. F. Janssens and F. S. Stephens, Nucl. Phys. News **6**, 9 (1996).
[12] M. Cromaz *et al.*, Nucl. Instrum. Methods Phys. Res., Sect. A **462**, 519 (2001).
[13] D. C. Radford, Nucl. Instrum. Methods Phys. Res., Sect. A **361**, 297 (1995).
[14] K. Starosta *et al.*, Nucl. Instrum. Methods Phys. Res., Sect. A **515**, 771 (2003).
[15] F. Meissner, H. Salewski, W.-D. Schmidt-Ott, U. Bosch-Wicke, and R. Michaelsen, Z. Phys. A **343**, 283 (1992).
[16] W.-D. Schmidt-Ott, H. Salewski, F. Meissner, U. Bosch-Wicke, P. Koschel, V. Kunze, and R. Michaelsen, Nucl. Phys. A **545**, 646 (1992).
[17] C. M. Baglin, Nucl. Data Sheets **109**, 2033 (2008).
[18] D. T. Joss *et al.*, Phys. Rev. C **68**, 014303 (2003).
[19] T. Hild, W.-D. Schmidt-Ott, V. Kunze, F. Meissner, C. Wennemann, and H. Grawe, Phys. Rev. C **51**, 1736 (1995).
[20] D. J. Hartley *et al.* (unpublished).
[21] K. Theine *et al.*, Nucl. Phys. A **548**, 71 (1992).
[22] R. Bengtsson and S. Frauendorf, Nucl. Phys. A **327**, 139 (1979); **314**, 27 (1979).
[23] P. Möller, J. R. Nix, W. D. Myers, and W. J. Swiatecki, At. Data Nucl. Data Tables **59**, 185 (1995).
[24] F. Dönau, Nucl. Phys. A **471**, 469 (1987).
[25] A. Bohr and B. R. Mottelson, *Nuclear Structure*, Vol. II (Benjamin, New York, 1975).
[26] D. R. Jensen *et al.*, Nucl. Phys. A **703**, 3 (2002).
[27] G. Schönwaßer *et al.*, Nucl. Phys. A **735**, 393 (2004).
[28] D. J. Hartley *et al.*, Phys. Rev. C **72**, 064325 (2005).
[29] J. Recht *et al.*, Nucl. Phys. A **440**, 366 (1985).
[30] H. J. Jensen *et al.*, Nucl. Phys. A **695**, 3 (2001).
[31] H. Carlsson *et al.*, Nucl. Phys. A **551**, 295 (1993).
[32] P. Bringel *et al.*, Phys. Rev. C **75**, 044306 (2007).
[33] R. A. Bark, A. M. Baxter, A. P. Byrne, P. M. Davidson, G. D. Dracoulis, S. M. Mullins, T. R. McGoram, and R. T. Newman, Phys. Rev. C **67**, 014320 (2003).
[34] S. Frauendorf, L. L. Riedinger, J. D. Garrett, J. J. Gaardhøje, G. B. Hagemann, and B. Herskind, Nucl. Phys. A **431**, 511 (1984).